HAL open science

Group 12 and 13 metal-alkenyl promoted generation of long-chain branching in metallocene-based polyethylene

Orlando Santoro, Lorenzo Piola, Karl Mc Cabe, Olivier Lhost, Katty den Dauw, Alvaro Fernandez, Alexandre Welle, Laurent Maron, Jean-François Carpentier, Evgueni Kirillov

To cite this version:

Orlando Santoro, Lorenzo Piola, Karl Mc Cabe, Olivier Lhost, Katty den Dauw, et al.. Group 12 and 13 metal-alkenyl promoted generation of long-chain branching in metallocene-based polyethylene. European Polymer Journal, 2022, 173, pp.111257. 10.1016/j.eurpolymj.2022.111257 . hal-04013388

HAL Id: hal-04013388

https://univ-rennes.hal.science/hal-04013388v1

Submitted on 3 Mar 2023

HAL is a multi-disciplinary open access archive for the deposit and dissemination of scientific research documents, whether they are published or not. The documents may come from teaching and research institutions in France or abroad, or from public or private research centers.

L'archive ouverte pluridisciplinaire **HAL**, est destinée au dépôt et à la diffusion de documents scientifiques de niveau recherche, publiés ou non, émanant des établissements d'enseignement et de recherche français ou étrangers, des laboratoires publics ou privés.

Distributed under a Creative Commons Attribution - NonCommercial 4.0 International License

Group 12 and 13 Metal-Alkenyl Promoted Generation of Long-Chain Branching in Metallocene-Based Polyethylene

Orlando Santoro,[a,†] Lorenzo Piola,[a,†] Karl Mc Cabe,[c] Olivier Lhost,[b] Katty Den Dauw,[b] Alvaro Fernandez,[b] Alexandre Welle,[b] Laurent Maron,[c,*] Jean-François Carpentier[a,*] and Evgueni Kirillov[a,*]

[a] Univ Rennes, CNRS, Institut des Sciences Chimiques de Rennes (ISCR), UMR 6226, F-35042 Rennes, France

[b] Total Research & Technology Feluy, Zone Industrielle Feluy C, B-7181 Seneffe, Belgium

[c] Université de Toulouse, CNRS, INSA, UPS, LPCNO, UMR 5215, 135 avenue de Rangueil, F-31077 Toulouse Cedex 4, France

† Those two authors equally contributed to this work.

* Correspondence to Laurent Maron (laurent.maron@irsamc.ups-tlse.fr), Jean-François Carpentier (jean-francois.carpentier@univ-rennes1.fr) and Evgueni Kirillov (evgueni.kirillov@univ-rennes1.fr).

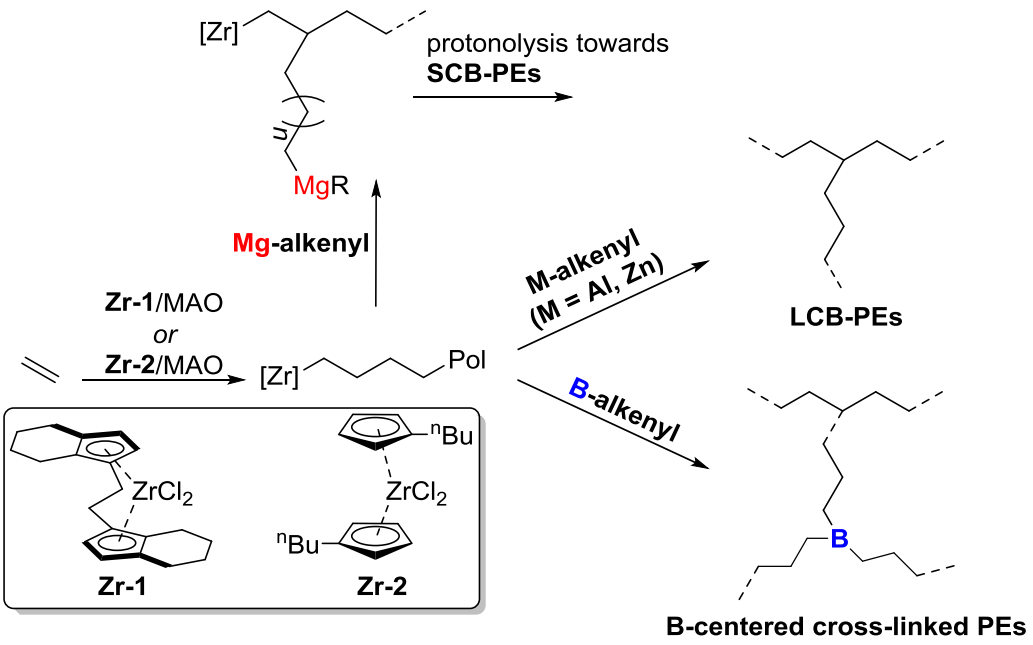

Abstract. *In situ* synthesis of topologically modified linear polyethylenes (PEs) using single-site polymerization catalysis is a challenging task that enables the production of advanced materials with tailored properties. We describe here our investigations aimed at an efficient generation of long-chain branches (LCB) in linear PEs using discrete B-, Al- and Zn-alkenyl co-reagents in combination with homogeneous *rac*-{EBTHI}$ZrCl_2$ (**1**)/ or (*n*BuCp)$ZrCl_2$ (**2**)/MAO catalytic systems. As corroborated by extensive rheological studies and ^{13}C NMR spectroscopy, Al-and Zn-based reagents promote LCB formation via a two-step mechanism involving both vinylic group insertion and M→Zr transmetallation steps. In striking contrast, the B-alkenyl species was found to form hydrolytically stable B-centred cross-linked PE structures. The Mg-based reagent appeared to be reluctant towards Mg→Zr transmetallation reaction, providing only the products of vinylic group insertion, which after hydrolysis afforded short-chain branched (SCB) PEs. The experimental observations were rationalized by DFT computations.

Introduction

The production of polyethylene (PE) with high molecular weight and narrow polydispersity has been largely enabled thanks to the development of single-site catalyst technology.[1] Although these characteristics confer excellent mechanical properties, such polymers suffer from poor processability due to their low elasticity and melt viscosity. Since the processing behaviour of PE is strongly dependent on its intrinsic properties such as molecular weight (M_w), polydispersity (M_w/M_n) and, more generally, its molecular architecture (linear, branched or cross-linked), it can be improved by introducing long-chain branching (LCB) to the linear PE structures.[2,3,4] Several post-reactor technologies have been reported to produce LCB-polymers: high-energy electron beam irradiation,[5] peroxide curing [6,7,8] and grafting.[9] However, due to the radical mechanisms involved in these treatments, ample control over LCB formation appeared to be impossible, and polymers exhibiting complex structures are obtained in those cases. Also, in-reactor technologies have been developed including copolymerization of ethylene with either *in situ*-formed or previously isolated macromonomers [10,11] or with a non-conjugated α,ω-diene.[12,13,14,15,16] For copolymerization techniques, only a limited number of catalysts have been found to efficiently generate and incorporate macromonomers. The second approach is limited by the rather scarce availability of α,ω-dienes and by the uneven distribution of LCB in the resulting polymers [17].

In recent studies, the Al-alkenyl compound *i*BuAl(oct-7-en-1-yl)$_2$ (**Al-1**) [18] has been successfully used as an LCB-promoter in the polymerization of ethylene catalyzed by homogeneous *rac*-{EBTHI}$ZrCl_2$ (**Zr-1**)/MAO and (*n*BuCp)$_2$$ZrCl_2$ (**Zr-2**)/MAO or their heterogeneous MAO on silica-supported-**Zr-1 or Zr-2**/TIBAL versions (EBTHI = ethylenebis(tetrahydroindenyl)).[19,20] Both experimental and computational techniques have identified the crucial role of **Al-1** co-reagent in the generation of LCB. In particular, it

has been corroborated that the two-step mechanism involves (1,2-) insertion of a pending oct-7-enyl moiety into the Zr–$C_{Polymeryl}$ bond, followed by Al→Zr transmetallation, eventually generating a growing polymer side-chain (Scheme 1). On the contrary, (incidental or final) protonolysis of the intermediate species would lead to the formation of *n*-hexyl short-chain branches (SCB). Although the discrimination between LCB and SCB in the final polymer could not be performed by means of ^{13}C NMR spectroscopy, [21,22,23] the use of this Al–vinyl transfer agent (AVTA) resulted in a marked change in the rheological behavior of the PEs, unambiguously consistent with LCB generation.

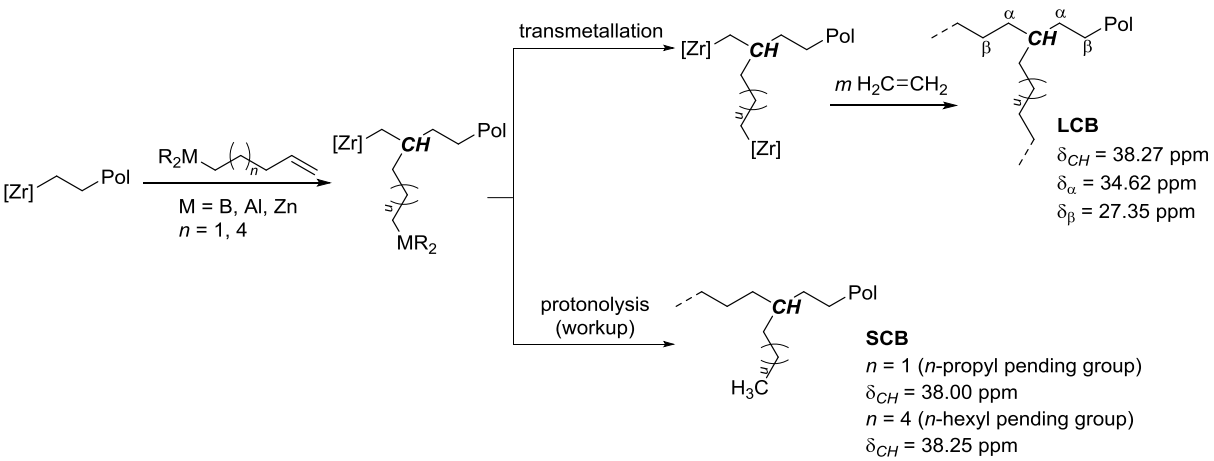

Scheme 1. Proposed pathway involving transmetallation and vinylic insertion steps, and ^{13}C NMR spectroscopic characterisation of short- (SCB) and long-chain branching (LCB) obtained in the presence of M–alkenyl co-reactants.[19]

To the best of our knowledge, this methodology remains widely unexplored and the reports in the open literature concerning the use of either Al-based reagents or other M–alkenyl compounds remain very scarce.[24,25] Herein, we report on the synthesis of LCB-PEs mediated by *discrete* B-, Al-, Mg- and Zn-alkenyl co-reagents, namely B(pent-4-enyl)$_3$ (**B-2**), Al(pent-4-enyl)$_3$ (**Al-2**), Mg(pent-4-enyl)$_2$ (**Mg-2**) and Zn(oct-7-enyl)$_2$ (**Zn-1**). The

shorter alkenyl group (pent-4-enyl) was selected to allow for the unambiguous detection of LCB by ^{13}C NMR spectroscopy. In fact, the resonance for the tertiary carbon at the branching point of LCB and those of the pendant alkyl groups arising from the insertion/protonolysis of the co-reagents could be hence easily discriminated, which was not possible in prior investigations. Additional information concerning the level of branching/cross-linking of the PE samples was achieved by means of melt rheology analysis. In turn, **B-2** proved to have a tremendous impact on the flow properties of the corresponding polymers.

Results and discussion

Synthesis of M-alkenyl reagents. Mg-, B- and Al-alkenyl reagents were prepared using modified literature protocols (Scheme 2). Zn(oct-7-enyl)$_2$ (**Zn-1**) was synthesised by chain-transfer from its parent boron analogue.[26] Mg(pent-4-enyl)$_2$ (**Mg-2**) and B(pent-4-enyl)$_3$ (**B-2**) were synthesised from the corresponding Grignard reagent by displacement of the Schlenk equilibrium with excess 1,4-dioxane and Mg-*to*-B transmetallation, respectively.[27,28] Al(pent-4-enyl)$_3$ (**Al-2**) was obtained by chain-transfer from the parent **B-2** onto trimethylaluminum.[29,30]

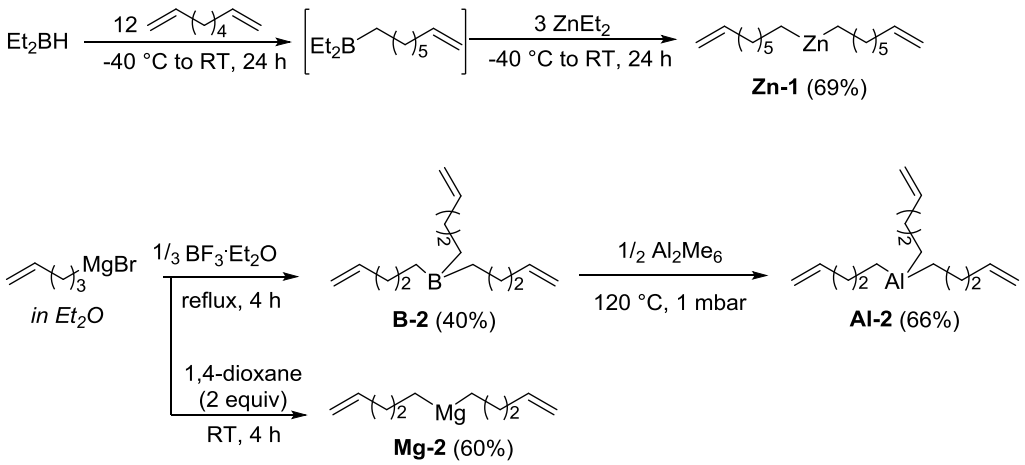

Scheme 2. Synthesis of putative LCB-promoting co-reagents B(pent-4-enyl)$_3$ (**B-2**), Al(pent-4-enyl)$_3$ (**Al-2**), Mg(pent-4-enyl)$_2$ (**Mg-2**) and Zn(oct-7-enyl)$_2$ (**Zn-1**).[27–29]

Polymerization of ethylene catalyzed by homogeneous *rac*-{EBTHI}$ZrCl_2$ and (*n*BuCp)$_2$$ZrCl_2$/MAO/M-alkenyl systems. Table 1 summarizes the ethylene polymerization experiments carried out using metallocene/MAO systems in the presence of the M-alkenyl co-reagents. The Zr-based pre-catalysts reported in Chart 1, namely *rac*-ethylenebis(4,5,6,7-tetrahydro-1-indenyl)]zirconium dichloride (**Zr-1**) and bis(*n*-butyl-cyclopentadienyl)zirconium dichloride (**Zr-2**), were employed in order to make a direct comparison with our previous works.[19] Such metallocenes were selected due to their opposite behaviour towards LCB formation. In fact, while **Zr-1** proved more prone to afford branched PEs by macromonomer insertion, **Zr-2** is known to lead mainly to purely linear polymers [31].

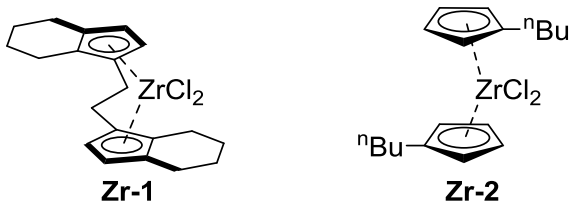

Chart 1. Structures of rac-{EBTHI}$ZrCl_2$ (**Zr-1**) and (nBuCp)$_2$$ZrCl_2$ (**Zr-2**).

For each catalytic system, reference reactions in the absence of M-alkenyl co-reactants (Table 1, entries 1 and 12) and in the presence of the previously investigated **Al-1** (Table 1, entries 2 and 13) were reported.[19] Compared to these benchmark runs, a positive effect on the polymerization productivity was observed upon introducing **Zn-1**, **Mg-2** and **Al-2**. With the **Zr-1**/MAO system, a slight improvement of productivity was observed also in the case of **B-2** for B/Zr molar ratios of 50 and 200 (Table 1, entries 9 and 10); contrastingly, a significant drop was occurred when 500 equiv of co-reagent were employed (Table 1, entry 11). We assume that such a decrease could be due to monomer diffusion issues arising from the gelation of the reaction medium in the presence of high concentration of the co-reagent. On the other hand, when **B-2** was used in combination with **Zr-2**/MAO, no variation of

productivity was observed (Table 1, entries 20–22). In all cases, the polymers showed lower melting temperatures and broader molecular weight distributions compared to the reference materials **PE1** and **PE12**.[32, 33]

In order to assess the possible formation of LCB, the samples produced with **Al-2** (**PE8** and **PE19**) were analysed by ^{13}C NMR spectroscopy. No signals compatible with LCB were detected but a significant amount of *n*-propyl branches (11.0 and 5.3 /10,000C for **PE8** and **PE19**, respectively) was found (Figures S1−S3). For PE samples prepared with **B-2** (**PE10** and **PE22**), ^{13}C NMR spectroscopy analysis could not allow unambiguous identification of the signal from the *C*H group at the branching point (overlapping with other minor signals), but rather intense resonances assignable to the CH_2 fragments at the α- and β-position of the LCB branching point were clearly observed (Figures S4 and S5, respectively). The LCB content calculated from the area of those signals was found to be 1.9 and 2.5/10,000C for **PE10** and **PE22**, respectively. Several other unassigned signals, probably corresponding to more complex branched structures involving B-alkyl linkers, were also detected (*vide infra)*.

Table 1. Polymerization of ethylene with **Zr-1** or **Zr-2**/MAO/**Al-1,2 - Mg-2**, **B-2** or **Zn-1** systems. [a]

Entry	Sample ID	Complex	M-alkenyl [M/Zr, mol/mol]	Productivity [kg_{pol}/kg_{cat}]	T_m [b] [°C]	T_c [b] [°C]	M_w [c] [10^{-3}]	M_w/M_n [c]	LCB [d]	Crystallinity [e] [wt.%]
1[f]	**PE1**	**Zr-1**	none	8,750	136	118	141.2	3.3	0.3	48
2[f]	**PE2**		**Al-1** (500)	7,670	128	116	94.0	3.6	nd	37
3	**PE3**		**Zn-1** (50)	13,830	133	119	191.3	5.5	nd	55
4	**PE4**		**Zn-1** (200)	11,000	132	118	99.9	3.8	nd	49
5	**PE5**		**Zn-1** (500)	8,330	128	114	55.6	4.1	nd	46
6	**PE6**		**Mg-2** (50)	12,835	133	118	215.5	5.1	nd	58
7	**PE7**		**Mg-2** (200)	8,335	133	116	255.7	3.0	nd	43
8	**PE8**		**Al-2** (500)	11,610	130	117	146.7	3.5	0.0[g]	45
9	**PE9**		**B-2** (50)	10,670	132	117	169.2	4.3	nd	46
10	**PE10**		**B-2** (200)	9,850	130	116	144.8	4.3	1.9[h]	44
11	**PE11**		**B-2** (500)	2,340	128 120	118 107	Insoluble		nd	32
12[i]	**PE12**	**Zr-2**	none	10,500	134	119	108.7	3.6	0.5	41
13[i]	**PE13**		**Al-1** (500)	10,800	129	115	116.0	4.1	nd	37
14	**PE14**		**Zn-1** (50)	10,500	133	118	106.5	4.7	nd	50
15	**PE15**		**Zn-1** (200)	14,470	133	118	114.9	3.5	nd	45
16	**PE16**		**Zn-1** (500)	15,000	132	118	80.4	4.0	nd	52

17	**PE17**	**Mg-2** (50)	10,000	134	118	161.7	2.9	nd	49
18	**PE18**	**Mg-2** (200)	11,335	133	118	122.7	2.9	nd	49
19	**PE19**	**Al-2** (500)	14,835	132	117	112.1	3.0	0.0[g]	50
20	**PE20**	**B-2** (50)	10,200	134	119	127.9	3.6	nd	48
21	**PE21**	**B-2** (200)	10,500	133	118	175.8	4.4	nd	43
22	**PE22**	**B-2** (500)	11,200	132	118	133.0	6.1	2.5[h]	52

[a] Reaction conditions: [Zr] = 10 μM, Al_{MAO}/Zr = 5,000, T = 60 °C, 15 min, Toluene = 150 mL, $P_{ethylene}$ = 4 barg; [b] Determined by Differential Scanning Calorimetry (DSC); [c] Determined by Size Exclusion Chromatography (SEC); [d] Determined by ^{13}C NMR spectroscopy calculated form the area of the signal from the *C*H group at the branching point, unless otherwise stated; [e] Calculated from [($\Delta H_m/\Delta H^0_m$) × 100], where ΔH_m is the heat of fusion of the sample (in J/g) determined by DSC and ΔH^0_m is the theoretical heat of fusion for 100% crystalline PE (293 J/g);[34] [f] Data from ref. [19]; [g] Only *n*-propyl branches were detected; [h] Potential LCB calculated from area of the CH_2 (α) and CH_2 (β) signals; [i] Data from ref. [20]

.

The effect of the M-alkenyl co-reactants on the rheological properties of the PEs was next investigated. The van Gurp-Palmen plots of the samples prepared with the **Zr-1**/MAO system were all indicative of LCB-PEs (Figure 1). In fact, all curves tend (at low |G*|) to phase angles (δ) lower than 90 °, that is the values found for purely linear polymers.[35,36,37] **PE3**, isolated in the presence of 50 equiv of **Zn-1**, described a curve almost superimposable to that of **PE2**, the benchmark sample obtained with a greater concentration of **Al-1** (500 equiv). A significant drop of phase angle, indicative of higher LCB-density, was also observed with **PE4** (200 equiv of **Zn-1**). However, the extent of branching drastically dropped for higher **Zn-1**/Zr ratios (**PE5**).[38] **PE6** and **PE7**, prepared with **Mg-2**, exhibited the same rheological behavior as the reference sample **PE1**, indicating no effect of such co-reagent as LCB-promoter. The samples produced with **Al-1** and **Al-2** (**PE2** and **PE8**, respectively) displayed an almost identical rheological response, suggesting no effect of the length of the alkenyl chain on the extent of LCB. Remarkably, a drastic drop of phase angle δ consistent with the amount of B-alkenyl employed and accountable to LCB/crosslinking was observed for the PEs synthesized in the presence of **B-2** (**PE9** and **PE10**). Similar rheological fingerprints were detected for the samples obtained with the **Zr-2**/MAO catalytic system in combination with **Al-2**, **Mg-2** and **B-2**, while no effect of **Zn-1** was observed (Figure 2). Interestingly, for all curves, inflection points (*minimum*), further indicative of LCB/crosslinked structures, were observed at lower |G*| values.[39,40]

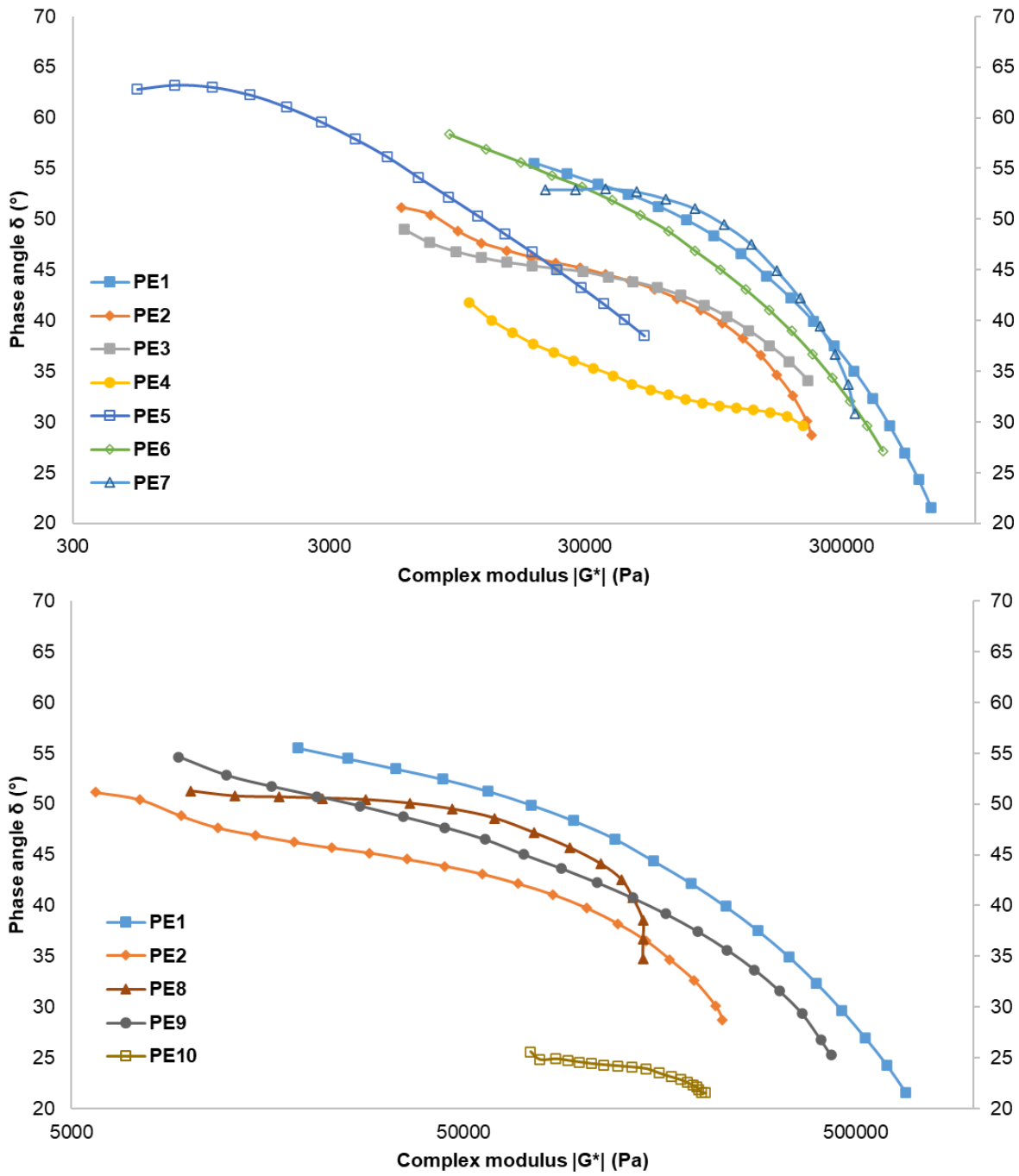

Figure 1. Van Gurp-Palmen plots for the PEs synthesised in the presence of M-alkenyl co-reactants with the catalytic system **Zr-1**/MAO (**PE1** and **PE2** reference samples).[19] Shear strain (γ) 10%, angular frequencies (ω) from 0.1 to 250 rad·s^{-1}, T = 190 °C, N_2 atmosphere.

Notably, for both catalytic systems, a significant deviation from the linear behaviour was obtained even for a [**B-2**]/[Zr] ratio of 50 (cf. **PE1**/**PE9** and **PE12**/**PE20**). For the sake of completeness, it is noteworthy that the drop of phase angle observed on the van Gurp-Palmen

plots could also be caused by the broadening of the molecular weight distribution. However, the presence of LCB was confirmed by the higher viscosities at low frequency (from 0.19 to 11 MPa·s and from 0.090 to 0.8 MPa·s for **PE1**/**PE9** and **PE12**/**PE20**, respectively) and pronounced shear thinning observed on the |η*|=f(ω) curves (Figures S6 and S7, respectively). Hence, the change of rheological behaviour could be imputed confidently to a combination of LCB and M_w/M_n broadening effects.

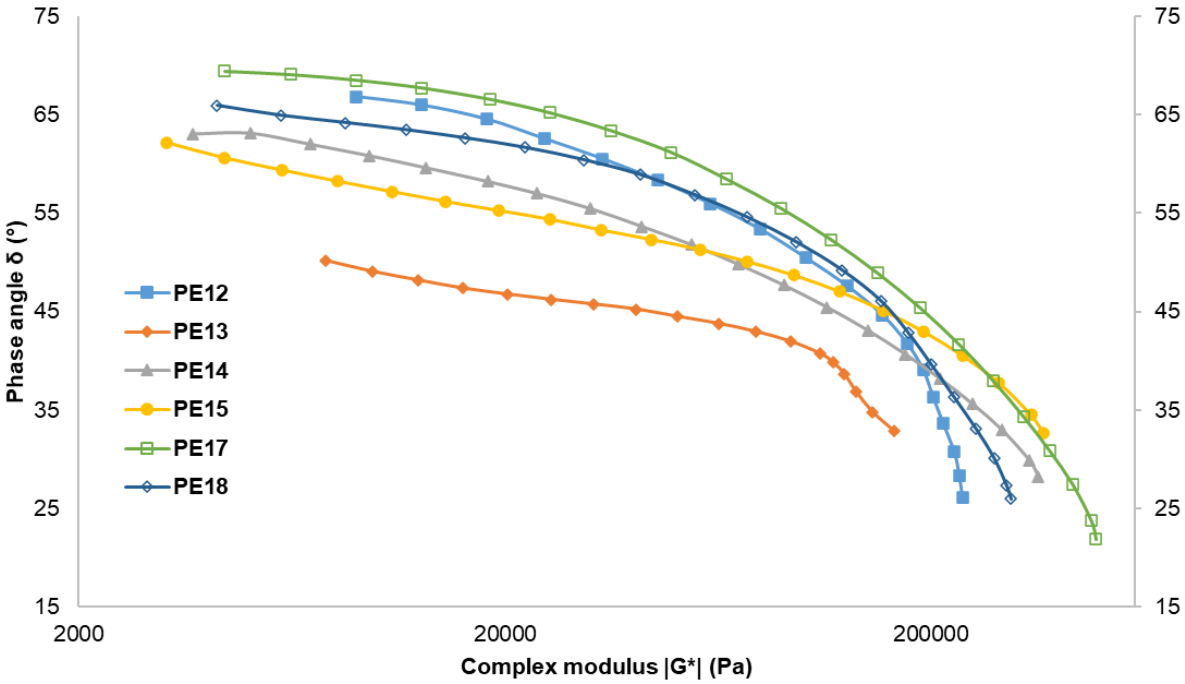

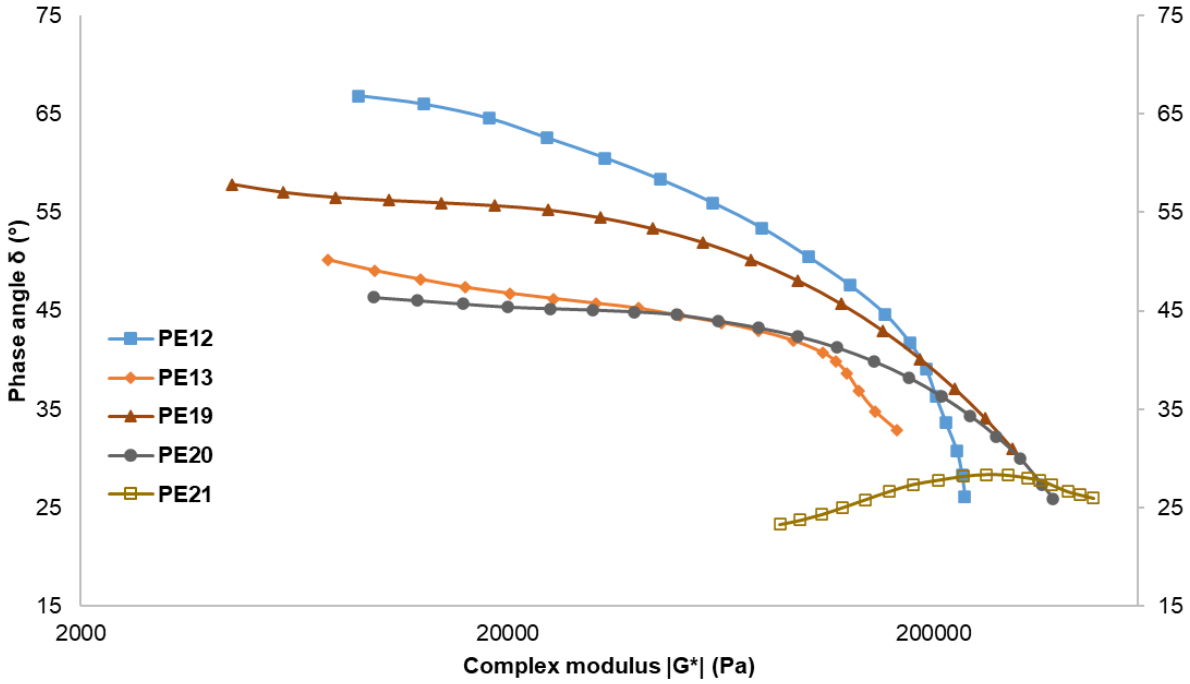

Figure 2. Van Gurp-Palmen plots for the PEs prepared in the presence of M-alkenyl co-reagents with the catalytic system **Zr-2**/MAO (**PE12** and **PE13** reference samples).[19] Shear strain (γ) 10%, angular frequencies (ω) from 0.1 to 250 rad·s^{-1}, T = 190 °C, N_2 atmosphere.

Overall, the NMR and rheological data shown above clearly suggests that **B-2** could be considered as the best LCB-promoter (or cross-linking agent, *vide infra*) of the series. In the first place, we hypothesized that chain transfer from B to Zr could be more favoured compared to the other M→Zr (M = Mg, Al, Zn) transmetallation, eventually leading to higher LCB densities. Nevertheless, the formation of B-containing branched/crosslinked architectures cannot be ruled out to account for the observed change in rheological behavior (

Scheme *3*); indeed, in contrast to the well-known ready protonolysis of Al–C bonds (that occurs during final hydrolytic workup), B–C cleavage does not readily occur under acidic conditions.[41,42,43] In order to corroborate this last hypothesis, **PE10** sample, synthesized with **Zr-1**/MAO system in the presence of 200 equiv. of **B-2** (Table 1, entry 10),

was treated with an aqueous base under harsh conditions in attempting to promote effective hydrolysis of B–$C_{polymeryl}$ bonds allegedly present in the PE structure (see the Supporting Information).

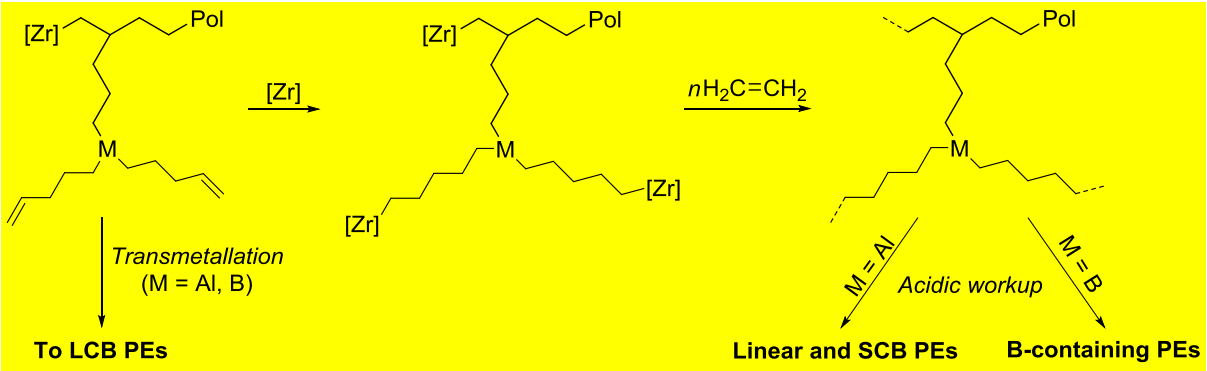

Scheme 3. Hypothetic pathway towards LCB-PEs containing B-alkyl moieties.

Compared to the parent material, higher melting and crystallization temperature values were obtained (133 vs 130 °C and 119 vs 116 °C, respectively). In addition, an interesting change in the rheological behaviour was also observed. In fact, the curve on the van Gurp-Palmen plot for the base-treated PE tends to a higher phase angle than that of the starting polymer (45 ° and 25 °, respectively) and similar to that of **PE2**, prepared with 500 equiv of **Al-1** (Figure 3). Moreover, the alkali-treated polymer exhibited lower viscosity al low frequency and lesser pronounced shear thinning than the parent sample (Figure S8). These observations are compatible with the drop of LCB-content caused by the base-treatment of the polymer and reinforce the hypothesis of the presence of branched or even cross-linked structures involving B–alkyl linkers.

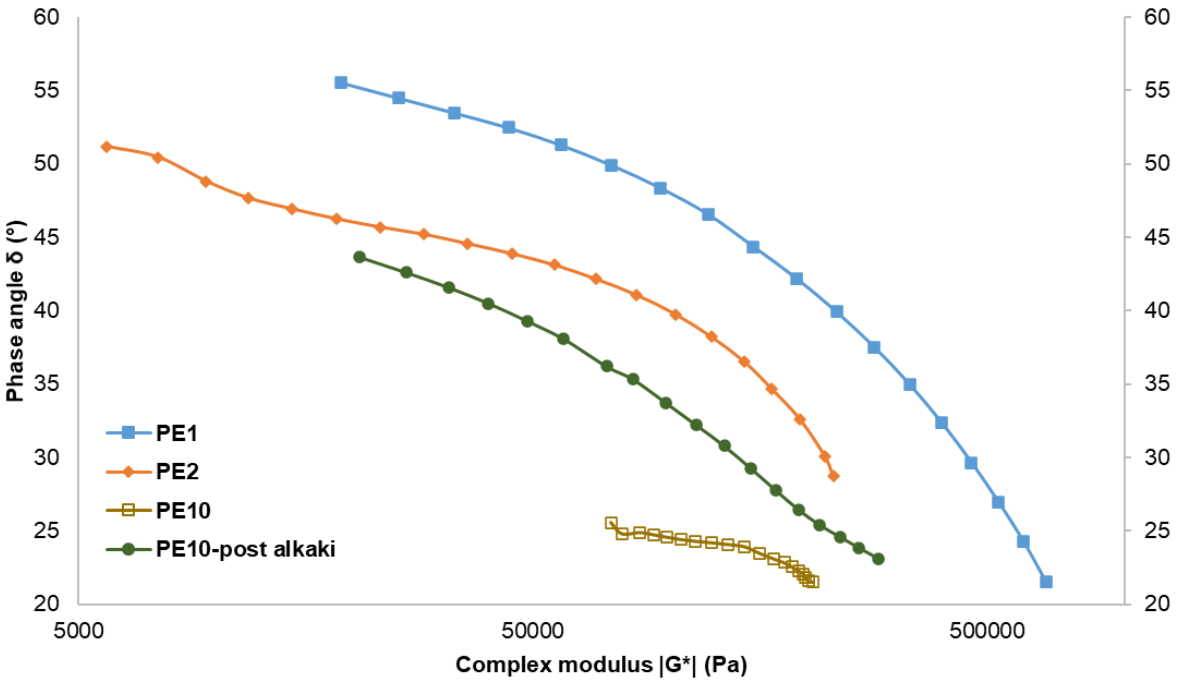

Figure 3. Comparison between the van Gurp-Palmen plots of **PE1**, **PE2** and **PE5** (before and after the alkaline treatment). Shear strain (γ) 10%, angular frequencies (ω) from 0.1 to 250 rad·s^{-1}, T = 190 °C, N_2 atmosphere.

Attempts to corroborate this supposition by ^{11}B NMR spectroscopy (both in solution and in the solid state) were unfortunately unsuccessful (see the Supporting Information, Figures S9–S11). On the other hand, Ion Beam analyses (IBA) confirmed the presence of boron in **PE10** and **PE22** and indicated a significant drop of the B-content as the result of the alkaline treatment of the former sample (see the Supporting Information, Figure S12 and Table S1).

DFT studies on the LCB formation with Zr-1 system in the presence of M-1,2 co-reagents. We next aimed at rationalizing the mechanism of formation of long-chain branches during polymerization of ethylene with **Zr-1** system, in the presence of M-alkenyl compounds (M = Al, B, Zn and Mg), by theoretical computations of the first, second and third insertion steps. The purpose of this study was to analyze the various coordinated co-catalyst – catalyst species and examine the change in structure as subsequent insertions of ethylene continue.

The focus of the DFT study is separated into three main aspects that allow insight into the nature of the bonding between co-reagent and catalyst systems: the coordination affinities to the catalyst system, the ability of this to influence subsequent ethylene insertions, and the possible insertion pathways generated by introduction of such co-reagents.

Previous investigations reported have eluded the way in which an Al-alkenyl moiety (**Al-1**) coordinates to catalyst systems [**Zr-1,2–R**]$^+$ (derived either from the neutral **Zr-1** or **Zr-2**), and the subsequent influences on the mechanisms of insertion by presenting a competitive coordination environment.[19] The following study thus began by examining the coordination affinities when computed M-alkenyl bridged heterobimetallic complexes are formed. This is compared initially with the coordination of ethylene monomer and both **B-2**, Mg(oct-7-enyl)$_2$ (**Mg-1**), and **Zn-1** species to the [**Zr-1–R**]$^+$ catalyst system (Table 2).

Table 2. The various coordination affinities of the co-reagents to the [**Zr-1–R**]$^+$ catalyst resulting in heterobimetallic Zr/M species.

[Zr-1–R]$^+$	**Coordination Energies (kcal·mol^{-1})**				
R	**Ethylene**	**Al-1**	**Mg-1**	**B-2**	**Zn-1**
Methyl	–2.4	–4.8	–17.9	11.3	–1.7
Propyl	–2.6	–5.0	–19.2	13.8	–3.0
Pentyl	1.0	–3.0	–7.9	15.8	–1.2

The coordination energies reported demonstrate two key points: (1) the addition of the M-alkenyl (M = Al or Zn) species tends to introduce a competitive coordination environment to the monomer (notice –2.4 vs. –4.8 and –1.7 kcal·mol^{-1}); (2) the **B-2** co-reagent seems to be destabilizing in the sense a heterobimetallic coordination through an alkenyl bridge and is unlikely here, contrasted by the strong stability offered by the **Mg-1** co-catalyst (–17.9 kcal·mol^{-1}). Understanding the coordination affinity between M–alkenyl and [**Zr-1–R**]$^+$ catalyst provides key insights toward the ability of these co-reagents to influence the possible

mechanisms of propagation. To clarify the extent to which either **Al-1**, **Zn-1** or **B-2** moieties impact the polymerization, investigations into the insertion mechanisms were next conducted.

Experimentally, an **Zr-1**/MAO/**M**(Al and Zn)-alkenyl environment appeared to promote LCB formation via the proposed insertion/transmetallation mechanism.[19] Computationally we observed a clear agreement with our reference **Zr-1**/MAO/**Al-1** polymerization condition, which has been reported as a beneficial mixture for LCB.[19,20] The two **Zn-1** and **B-2** co-reagents may promote the formation of LCB but, via the aforementioned investigations into their coordination affinity with the [**Zr-1–R**]$^+$ system, this may highlight a difference in the action to which a branched structure is formed. The **Zn-1** co-reagent follows a similar coordination trend to that of the reference **Al-1** co-reagent studied previously, highlighting a competitive coordination environment for either **Zn-1** or ethylene monomer about the [**Zr-1–R**]$^+$ catalyst. In contrast, the **B-2** co-reagent offers no initial competition to the monomer through an alkenyl-bridged coordination, suggesting an 'exclusive' preference to coordinate and insert a terminally located vinyl group on the co-catalyst ligand chain. This step would indicate a competition directly to form a branched polymer.

In agreement with experimental results, the ability of the **B-2** co-reagent to infer some competition toward a monomer coordination remains true regardless of increasing chain length on the [**Zr-1–R**]$^+$ catalyst. To examine how this affects the various mechanisms of insertions, a comparison can therefore be investigated through the insertion of a monomeric species to favour a linear chain growth vs. the insertion of a vinyl group on the **B-2** co-reagent which may allow the generation of LCB (Figure 4). The reactivity profile demonstrates the preference of the **B-2** system to coordinate through the vinyl group species (stabilizing the [**Zr-1–pentyl**]$^+$ catalyst by 4.2 kcal·mol^{-1}) rather than an alkenyl bridge (+15.8 kcal·mol^{-1}). This profile then nicely demonstrates the kinetic ability of this **B-2** co-reagent to generate a

competitive insertion environment about the catalyst to form a B-cross-linked PE product. Note that the transition states calculated between both co-reagent and monomer are almost identical (6.0 and 6.1 kcal·mol^{-1}, respectively). The formation of cross-links in this **B-2**/**Zr-1** environment is therefore considered highly plausible computationally. Recalling Figure 2 and samples **PE13**/**PE20**, the presence of the **B-2** co-reagent promotes the presence of branched or even cross-linked structures involving B-alkyl linkers. Through our DFT analysis, the formation of a stabilizing adduct at longer chain lengths, as well as a competitive insertion barrier with ethylene monomer, strongly supports the notion that the **B-2** co-reagent is capable of promoting branched or even cross-linked structures through aggregated vinyl group coordination and insertion steps in **Zr-1**-catalyzed environments.

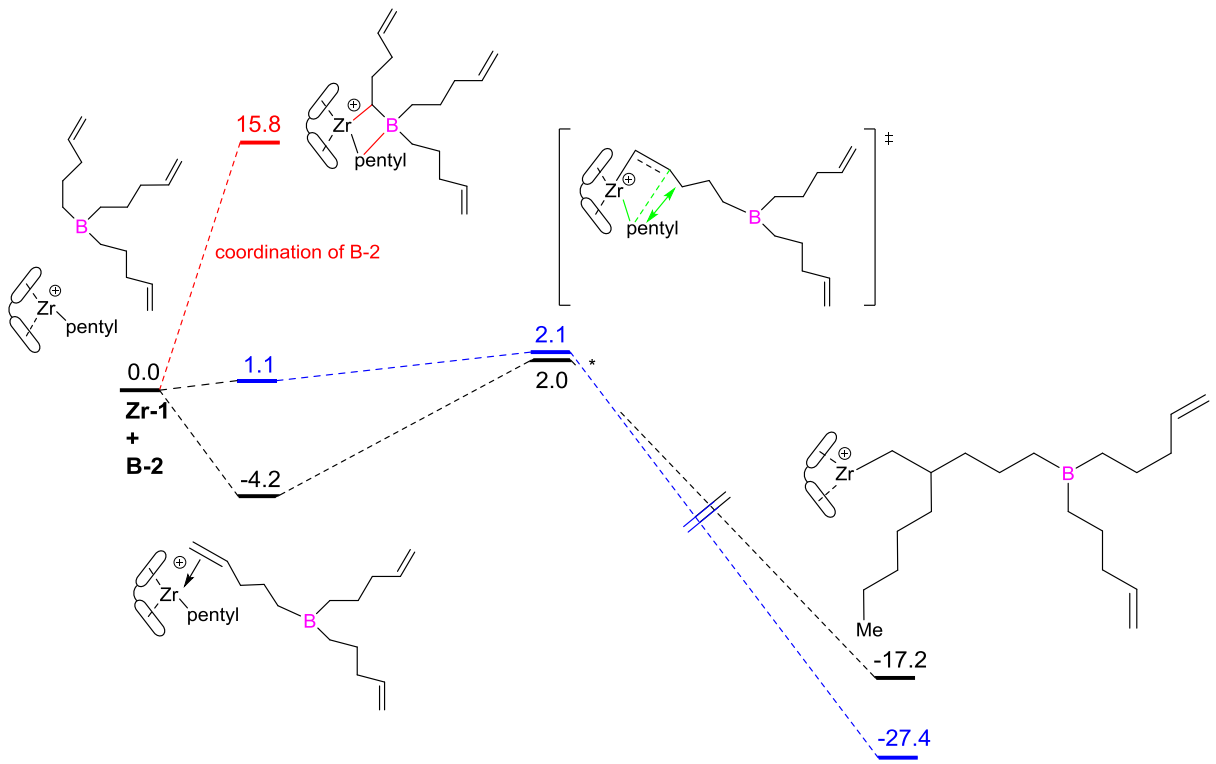

Figure 4. A comparison between the third coordination of either (a) the co-catalyst (red), (b) ethylene monomer (blue) or (c) the vinyl group from the co-catalyst pent-4-en-1-yl chain.

The same analysis, conducted on a **Zn-1** co-reagent system, presents the same observable trends: a stabilizing adduct and competitive insertion barrier to that of a monomer

insertion (Figure 5). Thus, computationally, it is evident that this co-catalyst system would induce LCB formations. Recalling the rheology patterns observed in Figure 1 also demonstrated that the **Zn-1**/**Zr-1** environments almost superimposed the same rheological fingerprint as the **Al-1**/**Zr-1** ratio at higher **Al-1** loadings, which would suggest a similar action of LCB formation. The profile below thus demonstrates a similar reactivity to promote LCB formations observed in **Al-1** environments.

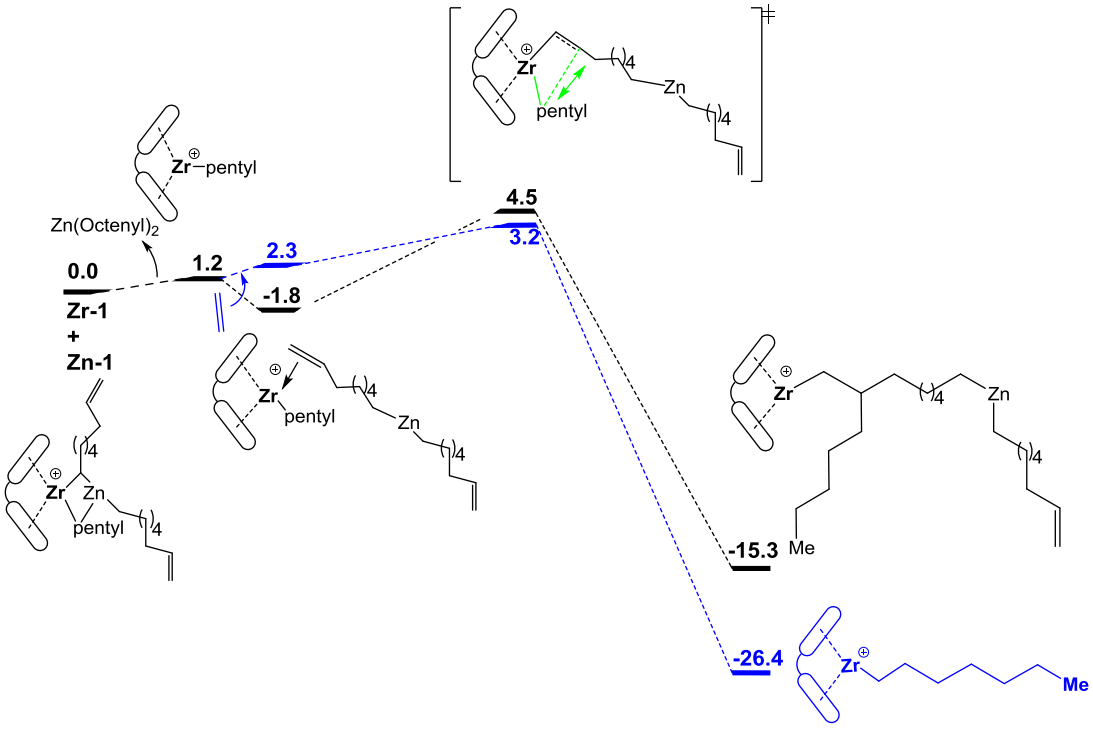

Figure 5. A comparison between the third coordination and insertion of either (a) the vinyl group from the **Zn-1** co-catalyst (black) and (b) ethylene monomer (blue).

The **Mg-1** compound offers a stabilizing coordination interaction to the **Zr-1** catalyst compared to ethylene monomer (–2.4 (monomer) vs –17.9 kcal·mol^{-1}). The stability of this coordination originates from the fact that the coordination itself is not a 'four-centered' heterobimetallic complex as we have previously observed in the other **Zr**/**M**-alkenyl systems. Instead, the **Mg-1** donates an oct-7-en-1-yl chain to the catalyst. The extent to which this coordination influences subsequent propagations was thus investigated considering a

transmetallation step and compared to a more general monomer coordination and insertion (Figure 6). The stability of the alkylation was considered via a monomer insertion into a Zr–$C_{alkenyl}$ bond, presenting a kinetic barrier of 24.9 kcal·mol^{-1}. This highlights the ability of propagation to continue at longer chain lengths after one step. The figure presented compares both an insertion pathway after a transmetallation event or dissociation of the **Mg-1** co-reagent, demonstrating the competitive kinetic environment between either insertion pathway or product formed. Interestingly, the insertion product after a transmetalation step seems to be thermodynamically favorable. This may offer an insight toward the reduced effects of LCB promotions: recalling samples **PE6** and **PE7** compared to that of the reference **PE1** (Table 1), whereby a **Mg-1** co-reagent has no effect on LCB rheologies; without hindering ethylene polymerization.

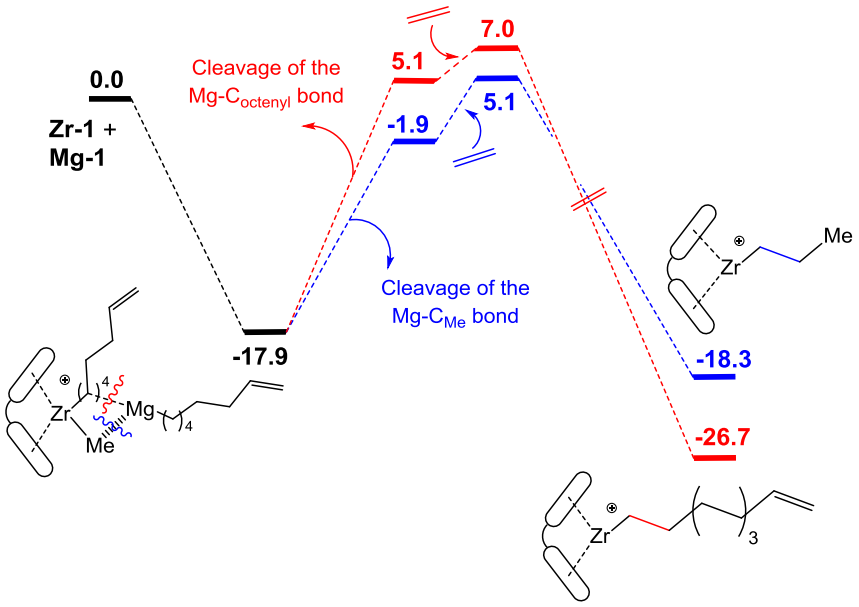

Figure 6. The coordination of **Mg-1** to [**Zr-1–Me**]$^{+}$, followed by the first insertion of ethylene via either cleavage of the Mg–$C_{alkenyl}$ or Mg–C_{alkyl} bonds. This profile illustrates the kinetic competition that is generated by the ability of a **Mg-1** co-catalyst to facilitate a transmetalation product after one insertion step.

LCB PE is thought to be produced via a vinyl group coordination and insertion from the co-reagent present in the reaction medium. Table 3 summarizes the coordination energies for the vinyl group on the various co-reagent systems toward the [**Zr-1–R**]$^+$ catalyst. Samples **PE6** and **PE7** indicate that, regardless of Mg-alkenyl concentrations, this co-reagent has little to no effect on LCB promotions. Computationally, this would rationalize an unfavored vinyl group coordination and insertion mechanism (+12.9, +13.2 and +3.4 kcal·mol^{-1}).

Table 3. The various vinyl coordination energies (in enthalpy) from an octenyl, or pentenyl chain from the co-reagent to the catalyst – R-moiety. Note that for the Mg, Al and Zn co-reagents, these are relative to the heterobimetallic species.

[**Zr-1–R**]$^+$	**Vinyl Coordination Energies (kcal·mol^{-1})**				
R	**Ethylene**	**Al-1**	**Mg-1**	**Zn-1**	**B-2**
Methyl	–2.4	–0.2	12.9	–3.0	–5.1
Propyl	–2.6	–0.4	13.2	–2.9	–6.6
Pentyl	1.0	–0.1	3.4	–3.0	–4.2

Conclusions

Discrete B-, Al-, Mg- and Zn-alkenyls have been synthesized and employed as LCB-promoters in the polymerization of ethylene catalyzed by **Zr-1** or **Zr-2**/MAO catalytic systems. The use of Al- and B-based co-reagents induced a clear change of the rheological behavior of the PEs compatible with LCB formation. This was much more evident for the samples prepared with the **Zr-1**/MAO system. On the other hand, the data collected for the B-derived branched PEs are in agreement with cross-linked structures incorporating hydrolytically stable B-centered branches, whose presence could be corroborated by ^{13}C NMR spectroscopy.

For the PEs obtained in the presence of **Zn-1**, the extent of branching appeared to be reduced drastically at higher Zn/**Zr-1** ratios. On the other hand, Mg- based co-reagents

appeared to be completely ineffective in combination with the given catalytic systems, likely due to the inability to promote the transmetallation step.

From a theoretical point of view, the observed trends computed are in agreement with the existence of a stabilizing interaction through the coordination of the co-reagent and monomer along with a kinetic insertion barrier that possibly could influence a monomer insertion (moving away from a classic linear polymer formation). The computations also highlighted the fact that changing the nature of the co-reagent indeed influences the mechanisms of insertion. M-alkenyl co-reagents generate LCB products through the initial formation of heterobimetallic adducts between the catalyst and co-reagent. Such an interaction allows the formation of a competitive environment about the catalyst, making an otherwise facile monomer insertion more dependent on the co-reagent presence and thus changing the propagative behavior. The **B-2** species both experimentally and computationally appears to promote B-centered cross-linked rather than LCB structures. This could be accounted to the failure of the B→Zr transmetallation due to the instability of the corresponding heterobimetallic B/Zr adducts.

Further synthetic and computational studies are currently under way to understand and use the potential of such co-reagents for the preparation of various tailor-made polymer architectures.

Acknowledgements: LM is a senior member of the Institut Universitaire de France. CalMip is acknowledged for a generous grant of computing time.

Funding sources: This work was gratefully supported by TotalEnergies One Tech Belgium (postdoctoral and PhD fellowships to OS, LP and KMC).

Appendix A: Supplementary data

Supporting information to this article (NMR spectroscopy and rheological analyses of polymers, computational details, Cartesian coordinates) can be found online at DOI:

References

[1] Alt, H. G.; Köppl, A. Effect of the Nature of Metallocene Complexes of Group IV Metals on Their Performance in Catalytic Ethylene and Propylene Polymerization. *Chem. Rev.* **2000**, *100*, 1205–1222

[2] Lai, S.-Y.; Wilson, J. R.; Knight, G, W.; Stevens, J. C.; Chum, P.-W. Elastic substantially linear olefin polymers U.S. Pat. 5,272,236, **1993** (to Dow Chemical co.).

[3] Brant, P.; Canich, J. A. M.; Dias, A. J.; Bamberger, R. L.; Licciardi, G. G.; Henrichs, P. M Long chain branched polymers and a process to make long chain branched polymers. WO 94/07930, **1994** (to ExxonMobil Chemical co.).

[4] Kim, Y. S.; Chung, C. I.; Lai, S. Y.; Hyum, K. S. Melt rheological and thermodynamic properties of polyethylene homopolymers and poly(ethylene/α-olefin) copolymers with respect to molecular composition and structure *J. Appl. Polym. Sci.* **1996**, *59*, 125–137.

[5] Rätzsch, M. Reaction mechanism to Long-Chain Branched PP. *J. Macromol. Sci. A.* **1999**, *36*, 1759–1769.

[6] Parent, J. S.; Bodsworth, A.; Sengupta, S. S.; Kontopoulou, M.; Chaudhary, B. I.; Poche, D.; Cousteaux, S. Structure–rheology relationships of long-chain branched polypropylene: Comparative analysis of acrylic and allylic coagent chemistry. *Polymer* **2009**, *50*, 85–94.

[7] Wang, X. C.; Tzoganakis, C.; Rempel, G. L. Chemical modification of polypropylene with peroxide/pentaerythritol triacrylate by reactive extrusion. *J. Appl. Polym. Sci.* **1996**, *61*, 1395–1404.

[8] Tian, J. H.; Yu, W.; Zou, C. X. The preparation and rheology characterization of long chain branching polypropylene. *Polymer* **2006**, *47*, 7962–7969

[9] Lu, B.; Chung, T. C. Synthesis of Long Chain Branched Polypropylene with Relatively Well-Defined Molecular Structure. *Macromolecules* **1999**, *32*, 8678–8680.

[10] Chum, P. S.; Kupper, W. J.; Guest, M. J. Materials Properties Derived from INSITE Metallocene Catalysts. *Adv. Mater.* **2000**, *12*, 1759–1767.

[11] Weng, W.; Markel, E. J.; Dekmezian, A. H. Synthesis of Long-Chain Branched Propylene Polymers via Macromonomer Incorporation. *Macromol. Rapid. Commun*. **2001**, *22*, 1488–1492.

[12] Kokko, E.; Pietikäinem, P.; Koivunen, J.; Seppälä, J. V. Long-chain-branched polyethene by the copolymerization of ethene and nonconjugated α,ω-dienes. *J. Polym. Sci.* **2001**, *39*, 3805–3817.

[13] Pietikäinem, P.; Väänänen, R.; Seppälä, J. V. Copolymerization of ethylene and non-conjugated dienes with Cp_2ZrCl_2/MAO catalyst system. *Eur. Polym. J.* **1999**, *35*, 1047–1055.

[14] Pietikäinem, R.; Seppälä, J. V.; Ahjopalo, L.; Pietilä, L.-O. Copolymerization of ethylene and non-conjugated dienes with Cp_2ZrCl_2/MAO catalyst system: effect of polymerization temperature on the copolymer structure. *Eur. Polym. J.* **2000**, *36*, 183–192.

[15] Naga, N.; Imanishi, Y. Copolymerization of Ethylene and 1,7- Octadiene, 1,9- Decadiene with Zirconocene Catalysts. *Macromol. Chem. Phys.* **2002**, *203*, 2155–2162.

[16] Williamson, A.; Fink, G. Alternating Copolymers of Ethylene and Diolefins Containing Pendent Functional Groups. *Macromol. Chem. Phys.* **2003**, *204*, 1178–1190.

[17] Das, C., Elguweri, M., Jiang, P., Kang, S., Kelchtermans, M., McLeish, T. C. B., Parkinson, M., Read, D. J., Redlich, M. P., Shirodkar, P. P., Soulages, J. M., Controlled Synthesis, Characterization, and Flow Properties of Ethylene–Diene Copolymers. *Macromol. React. Eng.* **2019**, *13*, 1800071–1800084.

[18] Holtcamp, M. W.; Day, G. S.; Hagadorn, J. R.; Palafow, O. J.; Mathiamagan, R.; Canich, J. M. Aluminum alkyls with pendant olefins for polyolefin reactions **2017** WO Pat. Appl. 2017039995 A1 (to ExxonMobil co.).

[19] Santoro, O.; Piola, L.; Mc Cabe, K.; Lhost, O.; Den Dauw, K.; Vantomme, A.; Welle, A.; Maron, L.; Carpentier, J.-F.; Kirillov, K. Long-Chain Branched Polyethylene via Coordinative Tandem Insertion and Chain-Transfer Polymerization Using *rac*-{EBTHI}$ZrCl_2$/MAO/Al-alkenyl Combinations: An Experimental and Theoretical Study. *Macromolecules* **2020**, *53*, 8847–8857.

[20] Santoro, O.; Piola, L.; Mc Cabe, K.; Lhost, O.; Den Dauw, K.; Vantomme, A.; Welle, A.; Maron, L.; Carpentier, J.-F.; Kirillov, E. Al-Alkenyl-Induced Formation of Long-Chain Branched Polyethylene via Coordinative Tandem Insertion and Chain-Transfer

Polymerization Using (nBuCp)$_2$ZrCl$_2$/MAO Systems: An Experimental and Theoretical Study. *Eur. Pol. J.* **2021**, *154*, 110567–110577.

[21] Stadler, F. J.; Piel, C.; Klimke, J.; Parkinson, M.; Wilhem, M.; Kaminsky, W.; Munstedt, H.; Influence of Type and Content of Various Comonomers on Long-Chain Branching of Ethene/α-Olefin Copolymers. *Macromolecules* **2006**, *39*, 1474–1482.

[22] Stadler, F. J. Detecting very low levels of long-chain branching in metallocene-catalyzed polyethylenes. *Rheol. Acta* **2012**, *51*, 821–840.

[23] Takeh, A.; Worch, J.; Shanbhag, S. Analytical Rheology of Metallocene-Catalyzed Polyethylenes. *Macromolecules* **2011**, *44*, 3656–3665.

[24] Lee, H. J.; Baek, J. W.; Kim, T. J.; Park, H. S.; Moon, S. H.; Park, K. L.; Bae, S. M.; Park, J.; Lee, B. Y. Synthesis of Long-Chain Branched Polyolefins by Coordinative Chain Transfer Polymerization. *Macromolecules* **2019**, *52*, 9311–9320.

[25] López-Barrón, C. R.; Lambic, N. S.; Throckmorton, J. A.; Schaefer, J. J.; Smith, A.; Raushel, F. N., Lin, T.-P. One-Pot Synthesis of High-Melt-Strength Isotactic Polypropylene Ionomers. *Macromolecules* **2022**, 55, 284–296.

[26] Chen, Y.; Clark, T. P.; Jazdzewski, B. A.; Klamo, S. B.; Wenzel, T. T. Synthesis of bis(7-octenyl)zinc via heterogeneous Ni catalysts. *Polyhedron* **2014**, *84*, 32–36.

[27] Belaid, I.; Poradowski, M.-N.; Bouaouli, S.; Thuilliez, J.; Perrin, L.; D'Agosto, F.; Boisson, C. Dialkenylmagnesium Compounds in Coordinative Chain Transfer Polymerization of Ethylene. Reversible Chain Transfer Agents and Tools To Probe Catalyst Selectivities toward Ring Formation. *Organometallics* **2018**, *37*, 1546.

[28] Lyle, R. E.; DeWitt, E. J.; Pattison, I. C. The Preparation and Properties of a Series of Ethereal and Unsaturated Boranes. *J. Org. Chem.* **1956**, *21*, 61–64.

[29] Koster, R.; Benedikt, G. Organic Aluminum Heterocycles. *Angew. Chem. Int. Ed.* **1962**, 1, 507.

[30] Dolzine, T. W.; Oliver, J. P. Intramolecular Metal-Double Bond Interactions. VI. Metal-π-Electron Interactions Observed in Trialkenylaluminum and -Gallium Derivatives. *J Am. Chem. Soc.* **1974**, *96*, 1737–1740.

[31] Kokko, E.; Malmberg, A.; Lehmus, P.; Löfgren, B.; Seppälä, J. V. Influence of the catalyst and polymerization conditions on the long−chain branching of metallocene–catalyzed polyethenes *J. Polym. Chem. Sci. A Polym. Chem.* **2000**, *38*, 376–388.

[32] The broadening of the molecular weight distributions could be accounted to the occurrence of alkyl exchange reactions between the main group element(s) and Zr

center (chain-transfer process); see for example: van Meurs, M.; Britovsek, G. J. P.; Gibson, V. C.; Cohen, S. A. Polyethylene Chain Growth on Zinc Catalyzed by Olefin Polymerization Catalysts: A Comparative Investigation of Highly Active Catalyst Systems across the Transition Series. *J. Am. Chem. Soc.* **2005**, *127*, 9913–9923.

[33] For entries 3-5 and 14-16, the possible occurrence of *in situ* alkyl exchange between **Zn-1** and $AlMe_3$ (from MAO) should also be considered. See: Wei, J.; Zhang, W.; Sita, L. R. Aufbaureaktion Redux: Scalable Production of Precision Hydrocarbons from AlR_3 (R=Et or *i*Bu) by Dialkyl Zinc Mediated Ternary Living Coordinative Chain-Transfer Polymerization. *Angew. Chem. Int. Ed.* **2010**, *49*, 1768–1772.

[34] Wang, S.; Wu, C.; Ren, M. Q.; Horn, R.M.V.; Graham, M.J.; Han, C.C.; Chen, E.; Chen, S.Z.D. Liquid-liquid phase separation in a polyethylene blend monitored by crystallization kinetics and crystal-decorated phase morphologies. Polymer **2009**, *50*, 1025–1033.

[35] Trinkle, S.; Friedrich, C.; Van Gurp-Palmen-plot: a way to characterize polydispersity of linear polymers. *Rheol. Acta* **2001**, *40*, 322–328.

[36] Trinkle, S.; Walter, P.; Friedrich, C. Van Gurp-Palmen Plot II – classification of long chain branched polymers by their topology. *Rheol. Acta* **2002**, *41*, 103–113.

[37] Ahmadi, M.; Rezaei, F.; Mortazavi, S. M.; Entezam, M.; Stadler, F. J. Complex interplay of short- and long-chain branching on thermal and rheological properties of ethylene/α-olefin copolymers made by metallocene catalysts with oscillating ligand structure. *Polymer* **2017**, *112*, 43–52.

[38] For **PE5**, the shift of the curve towards lower |G*| values was due to the lower M_w of the polymer compared to the other samples. This could indicate that for ratios [Zn]/[Zr] > 200 the co-reactant serves mainly as chain-transfer agent rather than as an LCB promoter.

[39] Stadler, F. J.; Chen, S.; Chen, S. On "modulus shift" and thermorheological complexity in polyolefins. *Rheol. Acta* **2015**, *54*, 695−704.

[40] Yan, Z.-C.; Stadler, F. J. Classification of thermorheological complexity for linear and branched polyolefins. *Rheol. Acta* **2018**, *57*, 377−388.

[41] Smith, K.; Pelter, A. "Hydroboration of C=C and C≡C" in *Comprehensive Organic Reactions*, **1991**, *9*, 703.

[42] Snyder, H. R.; Kuck, J. A.; Johnson, J. R. Organoboron Compounds, and the Study of Reaction Mechanisms. Primary Aliphatic Boronic Acids. *J. Am. Chem. Soc.* **1938**, *60*, 105–111.

[43] It has to be noted that B–C bonds, although hydrolytically stable, proved reactive towards atmospheric oxygen. See for example: Mirviss, S. B. The air oxidation of trialkylboranes. *J. Am. Chem. Soc.* **1961**, *83*, 3051–3056.